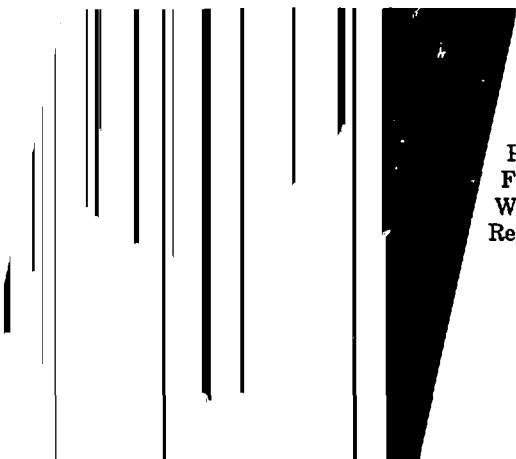


The Stability of Free-Electron Lasers Against Filamentation



J. J. Barnard, E. T. Scharlemann,
and S. S. Yu

September 15, 1987

Prepared for Ninth International
Free Electron Laser Conference,
Williamsburg, Virginia, Naval
Research Laboratory, Sept. 14-18, 1987

*Beam
Research Program*

DISCLAIMER

This document was prepared as an account of work sponsored by an agency of the United States Government. Neither the United States Government nor the University of California nor any of their employees, makes any warranty, express or implied, or assumes any legal liability or responsibility for the accuracy, completeness, or usefulness of any information, apparatus, product, or process disclosed, or represents that its use would not infringe privately owned rights. Reference herein to any specific commercial products, process, or service by trade name, trademark, manufacturer, or otherwise, does not necessarily constitute or imply its endorsement, recommendation, or favoring by the United States Government or the University of California. The views and opinions of authors expressed herein do not necessarily state or reflect those of the United States Government or the University of California, and shall not be used for advertising or product endorsement purposes.

The Stability of Free-Electron Lasers Against Filamentation*

J. J. Barnard, E. I. Scharlemann, and S. S. Yu
Lawrence Livermore National Laboratory, University of California
Livermore, CA 94550

UCRL--96821

I. Introduction

DE88 004712

In inertial confinement fusion (ICF) experiments, the high electromagnetic fields propagating through a relatively dense plasma can result in a transverse instability, causing the matter and light to form filaments oriented parallel to the light beam [1-5]. We examine whether a similar instability exists in the electron beam of a free-electron laser, where such an instability could interfere with the transfer of beam kinetic energy into optical wave energy.

In Section II we heuristically examine the instability in a relativistic beam through which an intense laser beam is propagating. We ignore the FFL effects (i.e., bunching of the electrons and the motion of the electrons through the wiggler). In Section III we estimate how the altered index of refraction (cf., refs. [6] or [7]) in an FEL affects the dispersion relation obtained in Section II. In Section IV we estimate the effect that the instability could have on the phase coherence of a particle as it transits an FEL.

II. Heuristic Estimate

The instability of a laser beam propagating through a plasma to transverse density perturbations can be qualitatively understood by the following arguments. In the frame in which the plasma is at rest, suppose a perturbation in density $\delta n'$ exists (say $\delta n' = \delta n'_0 \exp[ik'_\perp x']$) such that the perturbation wave vector k'_\perp is oriented perpendicular to the laser-beam wave vector k' , assumed parallel to the z-axis. In the comoving electron frame the index of refraction is $n'_r = (1 - (\omega'_p/\omega')^2)^{1/2}$. Here and throughout primes

DISTRIBUTION OF THIS DOCUMENT IS UNLIMITED

*Performed jointly under the auspices of the US DOE by LLNL under W-7405-ENG-48 and for the DOD under SDIO/-ATC MIPR No. W3TRPD-7-D4041.

MASTER

3/18

denote quantities in the comoving frame, ω'_p is the comoving plasma frequency, and ω' is the comoving laser frequency. Since n'_p is smaller in the high density region, the phase velocity of the laser is higher there so the laser will be refracted out, leaving a smaller electric field. The resulting low ponderomotive force in the high density region results in a higher density and thus the instability grows.

Quantitatively, the momentum equation is:

$$\frac{dv'}{dt'} \approx -\frac{1}{2\rho'} \left(\frac{\omega_p'}{\omega'} \right)^2 \frac{v}{8\pi} \frac{E'^2}{\rho'} - \frac{1}{\rho'} \frac{v}{8\pi} p' + \frac{e}{m} E'_s \quad , \quad (1)$$

where v is the fluid velocity, E is the laser electric field resulting in a ponderomotive pressure $1/2 (\omega_p'/\omega')^2 (E'^2/8\pi)$, p' is the comoving pressure, and E'_s is the electrostatic field due to the perturbation. If $\delta v'$, $\delta n'$, $\delta E'$, etc., are growing exponentially (e.g., $\delta n' = \delta n'_0 e^{\Gamma' t'}$), then Eq. (1), in the limit when ponderomotive pressure dominates, yields

$$\Gamma' \delta v' \approx \frac{-ik'}{m n'_0} \left(\frac{\omega_p'}{\omega'} \right)^2 \frac{E'_0 \delta E'}{8\pi} \quad , \quad (2)$$

where $\delta E'$ is the change in the electric field due to refraction by the density perturbation. Similarly the continuity equation relates $\delta v'$ to $\delta n'$ through

$$\frac{\delta n'}{at'} = -v \cdot n' v' \quad \Rightarrow \quad \Gamma' \delta n' \approx -k' n'_0 \delta v' \quad . \quad (3)$$

Thus Eqs. (1) and (3) imply

$$\Gamma'^2 \frac{\delta n'}{n'_0} \approx -\frac{c^2 k'^2}{2} \left(\frac{\delta E'}{E'_0} \right) a'_0^2 \quad , \quad (4)$$

where $a'_0 = eE'_0/m\omega'c$. In calculating the electric field response to the density perturbation, we note that in the regime in which the perturbation wavelength is long in a growth time (Γ'^{-1}) the rays will be refracted

away from the density peak a distance $\delta x' \ll 2\pi/k_1'$. Conservation of Poynting flux suggests $\delta E' \sim k_1' E'_0 \delta x'$. The ray trajectories are given by geometric optics where $dx_r'/dt = \partial\omega/\partial k_x$, $dk_x'/dt = -\partial\omega/\partial x$, (cf., [8]), which can be combined to give the ray trajectory:

$$\frac{d^2 x_r'}{dt'^2} = -\frac{c^2}{2} \left(\frac{\omega_p'}{\omega'} \right)^2 \left(\frac{1}{n_0'} \frac{\delta n'}{\delta x'} \right) . \quad (5)$$

Here x_r' is the x-coordinate of the ray and we have used the dispersion relation $\omega'^2 = c^2 k_1'^2 + \omega_p'^2$. In the long wavelength limit ($\Gamma' \gg k_1' dx_r'/dt'$) we assume the density perturbation obeys $\delta n' \sim \delta n'_0 e^{\Gamma' t'}$ and we try a ray trajectory of the form $x' = x'_0 + \delta x e^{\Gamma' t'} \sin k_1' x'_0$. This gives the approximate result

$$\delta x \approx \frac{k_1' c^2}{2\Gamma'^2} \left(\frac{\omega_p'}{\omega'} \right)^2 \frac{\delta n'}{n_0'} . \quad (6)$$

The resulting electric field perturbation thus satisfies

$$\frac{\delta E'}{E'_0} \approx -\frac{k_1'^2 c^2}{2\Gamma'^2} \left(\frac{\omega_p'}{\omega'} \right)^2 \frac{\delta n'}{n_0'} . \quad (7)$$

In the large k_1' regime, the growth time is much longer than a ray crossing time so that the density perturbation may be regarded as fixed, and the geometric optics equation becomes:

$$\frac{d^2(k_1' x_r')}{dt'^2} = \Omega^2 \sin k_1' x' ; \quad \text{where, } \Omega^2 \approx \frac{c^2 k_1'^2}{2\omega'^2} \omega_p'^2 \frac{\delta n'}{n_0'} \quad (8)$$

The rays oscillate back and forth about a density minimum like skiers making their way down a narrow chute.

At large k_1' , however, geometric optics is no longer strictly valid because diffraction effects become important. These tend to give any

ray a perpendicular velocity $v'_{\perp\text{diff}} \sim (ck'_1/\omega)c$, since the density perturbation acts like an aperture of diameter $2\pi/k'_1$. The refractive effects give perpendicular velocities $v'_{\perp\text{ref}} \sim \Omega/k'_1$. Analogous to the density of particles in a potential well with random velocities v'_{th} , we may expect the electric field (being proportional to the density of rays) to satisfy:

$$\frac{\delta E'}{E'_0} \sim -\frac{v'_{\perp\text{ref}}^2}{v'_{\perp\text{diff}}^2} \sim -\frac{\Omega^2 \omega'^2}{c^4 k_1^4} \sim -\frac{\omega_p'^2}{c^2 k_1'^2} \frac{\delta n'}{n'_0} . \quad (9)$$

Equation (9) may more rigorously be derived directly from the wave equation:

$$v'^2 E' - \frac{1}{c^2} \frac{\partial^2 (n'_r E')}{\partial t'^2} = 0 . \quad (10)$$

If $E'(x', y', z', t') = I^{1/2} \exp[ikS] \exp[ik'z' - \omega't']$, then substitute into Eq. (10) and linearize about a solution with temporally and spatially constant intensity I_0 and phase S_0 , we obtain the following equations for the linearized intensity I_1 and phase S_1 :

$$\frac{n'_r}{c} \frac{\partial I_1}{\partial t'} + \frac{\partial I_1}{\partial z'} = -I_0 v'^2 S_1 - \frac{4}{c} I_0 \frac{\partial \delta n'}{\partial t'} , \quad (11)$$

$$\frac{n'_r}{c} \frac{\partial S_1}{\partial t'} + \frac{\partial S_1}{\partial z'} = \frac{1}{4k'^2 I_0} v'^2 I_1 + \frac{\delta n'}{n'_r} . \quad (12)$$

If S_1 and $I_1 \sim e_1^{ik'_1 x' + \Gamma' t'}$, we find that

$$\frac{\delta |E'|}{E'_0} = \frac{1}{2} \frac{I_1}{I_0} = \frac{c^2 k_1^2}{2 \Gamma'^2 n'^2 r_0} \frac{\left[1 - 4 \Gamma'^2 n'^2 r_0^2 / (c^2 k_1^2) \right]}{\left[1 + c^2 k_1^4 / (4 \Gamma'^2 n'^2 r_0^2 k'^2) \right]} \frac{\delta n'}{n'_r} \quad (13)$$

For wave propagation in a uniform plasma,

$$\delta n'_r \approx -\frac{1}{2} \left(\omega_p'^2 / \omega'^2 \right) \left(\delta n' / n'_0 \right) . \quad (14)$$

In the limit $ck_1 \gg ck'_1$ ($k'_1/2k'$) $\gg \Gamma'$, to within factors of order unity, Eq. (9) is obtained, while if $ck_1 \gg \Gamma' \gg ck'_1$ ($k'_1/2k'$) then Eq. (7) is obtained. Combining the hydrodynamics (Eq. 4) with the field response Eqs. (7) and (9), yields:

$$\Gamma' \approx \begin{cases} ck'_1 \left(\frac{\omega_p}{\omega'} \right)^{1/2} a_0^{1/2} & \text{for } k'_1 \ll \frac{\omega'}{c} a_0^{1/2} \left(\frac{\omega_p}{\omega'} \right)^{1/2} \\ \left(\frac{1}{2} \right)^{1/2} a_0^{1/2} \omega' p & \gg \end{cases} \quad (15)$$

In the lab frame this corresponds to a spatial growth rate of:

$$\kappa \approx \frac{\Gamma'}{\gamma Bc} \approx \begin{cases} \frac{k_1}{\gamma^{3/4}} \left(\frac{\omega_p}{\omega} \right)^{1/2} a_0^{1/2} & \text{for } k_1 \ll \frac{a_0^{1/2}}{\gamma^{3/4}} \left(\frac{\omega_p}{\omega} \right)^{1/2} \frac{\omega}{c} \\ \left(\frac{1}{2} \right)^{1/2} \frac{a_0}{c} \frac{\omega_p}{\gamma^{3/2}} & \gg \end{cases} \quad (16)$$

Here all quantities are measured in the lab frame, $\omega_p^2 = 4\pi e^2 n_0 / m_e$, Bc is the parallel velocity ($\approx c$) and γ is the Lorentz factor. A more formal derivation based on a three wave interaction analysis [5] yields the same asymptotic results [10].

Although the above estimate ignores space-charge and thermal effects (which we will soon proceed to show act to stabilize the electron beam), the above formula should act as a rough upper limit to the growth rate. We compare the corresponding minimum growth length to the wiggler length in Table 1 for increasingly higher frequency and higher power FELs. It is apparent that progressively higher frequency FELs require larger Lorentz factors, which give effectively higher particle inertia and smaller growth rates. For comparison we list typical parameters from an ICF experiment. The growth rate can be much higher, since the plasma frequency can be higher, and more importantly the plasma is at rest, so $\gamma = 1$. (Note that in this column the ion-plasma frequency has replaced the electron-plasma frequency in calculating the growth length).

We may now consider the dispersion relation when the neglected terms in Eq. (1) are included. The third term arises because of space-charge effects. Using Poisson's equation, we obtain

$$E'_s \approx -i(4\pi e/k_{\perp})\delta n' \quad . \quad (17)$$

The second term represents thermal effects. Using an isothermal equation of state to represent the finite width of the velocity distribution (i.e., the finite emittance), the pressure gradient can be written:

$$\nabla p' \approx ik_{\perp} m c'_s^2 \delta n' \quad . \quad (18)$$

Here $c'_s = (aP/\delta p)^{1/2}$ is the sound speed in the comoving electron beam. Thus Eq. (4) should read (upon inclusion of thermal and space-charge effects):

$$\left[r'^2 + c'_s^2 k_{\perp}^2 + \omega_p'^2 \right] \frac{\delta n'}{n_0'} = - \frac{c^2 k_{\perp}^2 a_0'^2}{2} \frac{\delta E'}{E_0'} \quad . \quad (19)$$

When combined with (13) and (14) this yields the dispersion relation:

$$\left[r'^2 + c'_s^2 k_{\perp}^2 + \omega_p'^2 \right] = \frac{\left[c^2 k_{\perp}^2 k'^2 - 4r'^2 k'^2 n_0'^2 \right]}{\left[c^2 k_{\perp}^4 + 4r'^2 k'^2 n_0'^2 \right]} \frac{a_0'^2 c^2 k_{\perp}^2 \omega_p'^2}{2\omega'^2} \quad . \quad (20)$$

In the large k_{\perp} limit and in the lab frame this yields the spatial growth rate:

$$\kappa^2 \approx \left[\frac{a_0^2}{2} - 1 \right] \frac{\omega_p'^2}{\gamma^3} - c_s^2 k_{\perp}^2 \quad . \quad (21)$$

Here $c_s = c'_s/\gamma \approx c\epsilon/a$, where ϵ is the beam emittance and a is the radius of the electron beam. The growth rate κ becomes imaginary if $a_0^2 < 2$ or if the sound speed is sufficiently large, such that the sound transit time across the perturbation is shorter than the growth time in the absence of thermal effects. The three terms in Eq. (21) correspond to the ponderomotive, space-charge, and

thermal terms in the momentum equation, cf., Eq. (1). If ions had been present as they are in ICF applications, space-charge forces would be negligible because the ions would maintain charge neutrality at the relatively low frequency associated with filamentation and so the second term above would be absent. In an electron beam, however, there are no neutralizing particles so the self-electric fields of the perturbations prevent instability unless the laser field is very intense indeed. The required field for filamentation is larger than any present or proposed FEL.

III. FEL Effects

In Section II we investigated filamentation in a homogeneous relativistic electron beam. In an actual FEL, the electron beam is bunched and it undulates as it passes through the wiggler. We may estimate these effects by a consideration of the resulting index of refraction.

The dispersion relation for the signal wave in an FEL is (cf. [6]):

$$\frac{\omega^2}{c^2} - \frac{\omega_p^2}{\gamma_0 c^2} - (k + \phi')^2 = \frac{\omega_p^2 a_w^2}{c^2 a_0^2} \left\langle \frac{\cos \psi}{\gamma} \right\rangle \quad . \quad (22)$$

(In Eq. (22) we have set the imaginary part to zero; i.e. gain effects have been neglected.) Here $\langle \rangle$ denote averages over the period of the FEL ponderomotive potential well, with wavelength $2\pi/(k_w + k)$; ψ is the phase within the well; k_w is the wiggler wave vector; a_w is the amplitude of the wiggler vector potential, $a_w = eA_w/mc^2$; ϕ is the phase of the laser field; $a_s = a_0 \cos(kz - \omega t + \phi)$; and prime denotes the derivative with respect to z . The effective index of refraction is given by (cf. [7]):

$$n_r^2 \equiv c (k + \phi')^2 / \omega^2 = 1 - \frac{\omega_p^2}{\omega^2} \left[\frac{1}{\gamma_0} - \frac{a_w^2}{a_0^2} \left\langle \frac{\cos \psi}{\gamma} \right\rangle \right] \quad . \quad (23)$$

Since $\langle \cos \psi/\gamma \rangle$ is positive and on the order of $1/\gamma_0$, and since $a_w/a_0 \gg 1$ it is apparent that the phase velocity of the laser signal wave is largest where the density is smallest, a property which causes the wave fronts to tend to be focused into the beam (optical guiding, cf., ref. [7]). Thus if the density striations are perpendicular to the laser wave vector, regions of high density will tend to be regions of high field strength, opposite to that which is needed for filamentation.

We illustrate this quantitatively by redoing the estimate of Section II, using the altered index of refraction above.

In the large k_1 limit, we find that (in the lab frame) Eq. (13) yields:

$$\frac{\delta E}{E_0} \approx \frac{2k^2}{k_1^2} \delta n_r . \quad (24)$$

Perturbing Eq. (23) we find:

$$\delta n_r = - \frac{a_0 \omega_p^2}{2\langle \gamma \rangle \omega^2 n_0} \frac{\delta n}{n_0} - a_1 \frac{\delta E}{E_0} , \quad (25)$$

where

$$a_0 = 1 - \frac{\gamma_0 a_w}{a_0} \left\langle \frac{\cos \psi}{\gamma} \right\rangle \quad \text{and} \quad a_1 = \frac{\omega_p^2}{2\omega^2} \frac{a_w}{a_0} \left\langle \frac{\cos \psi}{\gamma} \right\rangle .$$

Using the lab frame equivalent of Eq. (2), i.e.,

$$\gamma^2 c^2 \kappa^2 \frac{\delta n}{n_0} \approx - \frac{c^2 k_1^2}{2} a_0^2 \frac{\delta E}{E_0} , \quad (26)$$

we find a spatial growth rate κ obeying

$$\kappa^2 \approx \frac{a_0}{2(1 + 2a_1 k_1^2/k_1^2)} \left(\frac{\omega_p}{c} \right)^2 \frac{a_0^2}{\gamma^3} . \quad (27)$$

The growth rate again becomes imaginary and so benign in the limit of large $\gamma_0 (a_w/a_0) \langle \cos \psi/\gamma \rangle$, even in the absence of space charge or thermal effects.

IV. Variation in Phase Due to Filamentation

Although our results indicate that growth of the instability is not likely to occur, high efficiency in the FEL requires that particles maintain their phase coherence (i.e., stay within the bucket) during the transit of the FEL. Perpendicular motions induced by the density perturbations could cause parallel velocity perturbations. We estimate an upper limit to the change in phase from these effects.

Equation (3) indicates that $\delta v \sim \kappa/k_{\perp} \delta n/n_0$. The phase $\psi = (k_w + k)z - \omega t$ implies that $\psi' = k_w - \kappa [1 + \gamma_0^2 \beta_{\perp}^2]/2\gamma^2$, ref. [6]. Thus the change in ψ' from the perturbation, $\Delta\psi' \sim \kappa \beta_{\perp}^2/2 \sim \kappa \beta_{\perp 0} \beta_s$. Using an upper limit on $\Delta v \sim \kappa/k_{\perp}$, an upper limit on $\kappa \sim \omega_p^3/\gamma^3 c$, and a lower limit on $k_{\perp} \sim 2\pi/a$ we find that $\Delta\psi' L = -k L \alpha_w \omega_p / (\gamma^{5/2} c k_{\perp})$, where L is the length of the wiggler. Table 11 lists these quantities for the three FELs of interest and finds that $\Delta\psi/2\pi \sim$ a few, for these upper limits. Thus we conclude if $\Delta n/n_0 \ll 1$, then $\Delta\psi \ll 2\pi$ and so phase variation will be negligible.

V. Conclusion

We have calculated the growth rate for filamentation of a relativistic beam in the presence of an electromagnetic wave propagating parallel to the beam. We find that space-charge and thermal effects prevent growth of filaments in such beams, if the velocities, densities, and laser field strengths are similar to those of current or proposed FELs. Our analysis indicates that the bunched and undulating beam in an actual FEL alters the index of refraction from that of a homogeneous beam such as to inhibit filamentation, although a more formal analysis is required to confirm this aspect. We also find that phase coherence of particles would be maintained, even if the instability occurred, unmitigated by space-charge, thermal, or FEL

effects. A somewhat more rigorous version of this work can be found in ref. [10].

References

1. Liang, E.P. and Langdon, A.B. (1987) Phys. Fluids, 30, 175.
2. Kaw, P., Schmidt, G. and Wilcox, T. (1973) Phys. Fluids, 16, 1522.
3. Chiao, R.Y., Garmire, E. and Townes, C.H. (1964) Phys. Rev. Lett. 13, 479.
4. Drake, J.F., Kaw, P.W., Lee, Y.C., Schmidt, G., Liu, C.S. and Rosenbluth, M.N. (1974) Phys. Fluids, 17, 778.
5. Schmidt, G. (1979) The Physics of High Temperature Plasmas (Academic Press: New York), Second Edition, Chapter IX.
6. Kroll, N.M., Morton, P.L., and Rosenbluth, M.N. (1981) IEEE J. Quant. Elec. QE-17, 1436.
7. Scharlemann, E.T., Sessler, A.M., and Wurtele, J.S. (1985) Nuc. Inst. Meth. Phys. Res. A239, 29.
8. Weinberg, S. 1962, Phys. Rev. 126, 1899.
9. Landau, L.D., and Lifshitz, E.M., (1959) Fluid Mechanics, (Pergamon Press: London), Chapter XV.
10. Barnard, J. J., Scharlemann, E. T., and Yu, S. S., Lawrence Livermore National Laboratory Research Memo (in preparation).

Table 1. Comparison of Growth Length with FEL Wiggler Length

Quantity	ETA (ELF)	ATA (PALADIN)	Higher Power FEL	"Typical" Laser- Target Parameters ICF
Current I (kA)	.8	3	3	
Energy γmc^2 (MeV)	3.5	50	300	$k_1 \sim 0.01$
Beam Radius a (cm)	0.6	0.5	0.2	
Peak Laser ($W cm^{-2}$) Intensity	10^9	10^{11}	10^{12}	10^{14}
Plasma Freq. ω_p Optical Freq. ω	0.09	3×10^{-4}	7×10^{-5}	0.2
Optical Freq. ω ($rad s^{-1}$)	2.4×10^{11}	1.8×10^{14}	2×10^{15}	2×10^{15}
Dimensionless a_0 Vector Potential	0.093	1.1×10^{-3}	6.15×10^{-4}	9×10^{-3}
Electric Field	$e_0 = k a_0 (cm^{-1})$	0.73	6.4	39
Wiggler Length	L (cm)	400	1500	10^4
Growth Length	$\frac{l}{\kappa}$ (cm)	180	3×10^5	3×10^6
				0.039*

(Also shown are comparable parameters for an ICF experiment.)

*The "wiggler length" has been replaced with $c \times$ (pulse time) and the "growth length" has been replaced with $c/\text{temporal growth rate}$ in the ICF column for comparison. Also, the ion plasma frequency replaced ω_p in calculating the growth rate in that column.

Table II: Maximum Change in Particle Phase Due to Filamentation

	ETA	ATA	High Power
k (cm $^{-1}$)	7.85	5.9×10^3	6.2×10^4
L (cm)	400	1500	10^4
$a_w/\sqrt{2}$	2.5	1.2	2.9
ω_p (rad s $^{-1}$)	2×10^{10}	5×10^{10}	1.2×10^{11}
γ	6.85	100	590
$k_{\perp min}$ (cm $^{-1}$)	10.5	12	31
$\frac{\Delta\psi_{max}}{2\pi}$	0.95	3.5	6.4